

Experimental study of the behavior of composite timber columns confined with hollow rectangular steel sections under compression

Leila Razavian¹, Morteza Naghipour¹, Mahdi Shariati^{*2,3} and Maryam Safa^{4a}

¹Civil Engineering Faculty, Babol Noshirvani University of Technology, Babol, Iran

²Division of Computational Mathematics and Engineering, Institute for Computational Science, Ton Duc Thang University, Ho Chi Minh City 758307, Vietnam

³Faculty of Civil Engineering, Ton Duc Thang University, Ho Chi Minh City 758307, Vietnam

⁴Institute of Research and Development, Duy Tan University, Da Nang 550000, Vietnam

(Received June 29, 2017, Revised October 5, 2017, Accepted November 27, 2019)

Abstract. There are separate merits and demerits to wood and steel. The combination of wood and steel as a compound section is able to improve the properties of both and ultimately increase their final bearing capacity. The composite cross-section made of steel and wood has higher hardness while showing more ductility and the local buckling of steel is delayed or completely prevented. The purpose of this study is to investigate the behavior of composite columns enclosed in wooden logs and the hollow sections of steel that will be examined in a laboratory environment under the axial load to determine the final bearing capacity and sample deformation. In terms of methodology, steel sheet and carbon fiber reinforced polymer sheet (FRP) are tested to construct hollow rectangular sections and reinforce timber. Besides, the method of connecting hollow sections and timber including glue and screw has been also investigated. As a result, timber lumber enclosed with carbon fiber-reinforced polymer sheets in which fibers are horizontally located at 90 ° are more resistant with better ductility.

Keywords: composite section; FRP; timber; bearing capacity; steel sheet

1. Introduction

Hollow rectangular steel sections have been used in China for 5 decades (Hosseinpour *et al.* 2018). In this case, they have been used as the main pillars of subway stations in Beijing since 1966 and applied in power plants since 1970. The use of these sections as a major compression system or key element of building and bridges has been recently increased (Han *et al.* 2007). Align with this, flexural behavior of concrete-filled steel beams have been numerously studied (Sinaei *et al.* 2011, Khanouki *et al.* 2016, Abedini *et al.* 2017, Shariati *et al.* 2018, Luo *et al.* 2019, Sajedi and Shariati 2019, Xie *et al.* 2019). The purpose of concrete-filled steel beams is to investigate the effect of slippage between the steel pipes on concrete core. In their study, the embedding of shear and confinement type are two key elements of variable. Accordingly, flexural strength, flexibility, failure mode, and cracking condition are the investigated parameters. A research by Lee *et al.* (2011) has examined the behavior of cold-rolled, thin-walled square columns with concrete core. The investigated parameters have included the strength of concrete, steel sections (sections of welded steel sections and typical profile) and the ratio of width to the thickness of steel wall. The effects of concrete on steel columns performance and on failure have been widely investigated (Gerami *et al.*

2008, Paknahad *et al.* 2018, Sedghi *et al.* 2018, Toghroli *et al.* 2018, Zhao *et al.* 2018, Mehrmashhadi *et al.* 2019). In 2009 de Oliveira *et al.* (2009) has conducted a study on the effect of confinement on CFT columns with circular sections under compressive axial load. In this study, the studied parameters have included concrete compressive strength and slenderness of columns. When the load reaches to the final concrete strength, fine cracks are increased and concrete side expansion is reached to its maximum value, thus from this moment the effect of concrete core confinement with steel has begun. The load-bearing capacity of columns is increased by the raise of 1) concrete core strength, and 2) slope of columns. Due to the poorly confined effect of steel structure for concrete core, their load-bearing capacity has been decreased. The scales have been examined by Zeghiche (2013) in a study of CFT columns with rectangular and I-shaped sections. Respectively, both of which are made from the connection of two curved U-shaped sheets. On the other hand, another parameters studied in this study have included column height, place and type of welding, steel cross-sectional shape, concrete core strength, and age. As a result, by the increase of column height, loading capacity is reduced which is noticeable for discontinuous weld parts. Compared to discontinuous welding, continuous welding has increased the lateral stiffness of columns while resulting a greater rupture resistance. By the increment of concrete-age which is used in CFT members, loading capacity has been also increased. Alternative materials for reinforcing structures have been recently focused on. Thus, polymeric coating of FRP has been initially developed in Europe and Japan in

*Corresponding author, Ph.D.

E-mail: shariati@tdtu.edu.vn

^a Ph.D.

E-mail: maryamsafa@duytan.edu.vn

1980s to improve the concrete structures (Austin 2003). A research by Eshaghian and Keramati (2017) have performed a research on concrete composite cylindrical columns of GFRP (glass fiber reinforced polymer), and analyzed the laboratory and Ansys numerical modeling. GFRP cylinder acts as on-site molding and provides concrete confinement. The results of experimental and numerical analysis have shown a high level of adaptability and consistency.

Another research by (Rashidi and Takhtfirouzeh 2018) have performed a laboratory research on concrete columns confined with GFRP sheets. After two-point bending load, a significant increase has been observed in bearing capacity of bending and shear reinforced concrete columns. In addition Chen *et al.* (2015) has used CFRP sheets to repair and reinforce the cracked hollow steel sections, and after three points loading, a significant increase in ultimate flexural strength has been observed. Also Ghanbari Ghazijahani *et al.* (2015) has studied new composites composed by rectangular steel sections filled with wood and confined with CFRP sheets. Composite wood and steel composite are lightweight and inexpensive that make it suitable to be used as a compression member with high resistance. The ultimate capacity of confined samples has been significantly improved and the local outward buckling has been prevented. This effect is longer when the short pillars are effectively confined with CFRP layers, and their outward buckling is prevented. [24] has repeated the same experiment by changing the shape of samples into cylinders while these samples are placed under pure axial load to measure the plastic buckling, rupture modes, and displacement. The increment of final capacity of each sample in different conditions and their behavior have been evaluated. The excessive increase in final load-bearing capacity of sample has been associated to the increased ductility. The benefits of confining wood in this way include 1) increasing resistance, 2) protecting wood against corrosion, 3) increasing the fire resistance and 4) preventing the wood cracking at very high temperatures. Basalt fibers are used as a reinforcement and concrete strength enhancer agent, also used as concrete bridge decks as corrosion resistant material. FRP-reinforced beams with high-temperature basalt fibers show a better behavior than FRP-reinforced beams with glass fibers. Today, FRP basalt rods are used to repair and reinforce wooden parts. A research by Raftery and Kelly (2015) have performed a pressure test on wooden samples reinforced with FRP basalt rods, resulting that these samples have better mechanical performance compared to the samples reinforced with FRP glass. Distance between neutral axis reinforcement has a special effect on the improvement of mechanical behavior of sample, and the continuity between wood and FRP basalt is consistent throughout the test.

Investigations have also been carried out to reinforce Glulam timbers, consisting of a number of layers of dimensioned lumber bonded together with durable and moisture-resistant structural adhesives.

Naghipour *et al.* (2011) has reinforced these beams by CFRP (carbon fiber reinforced polymer) and compared the data obtained from three methods of finite element, numerical and spectral method. It is concluded that the spectral method is the most appropriate method to

determine the dynamic properties and natural frequency of these beams. Taheri *et al.* (2005) has reviewed GLULAM beams (glued laminated timber) analysis and experimental tests of reinforced beams with GFRP sheets that prevented from breakage after reinforcement. It is found that increasing the number of reinforcing layers has a positive effect on the improvement of static resistance and natural frequency. In order to determine the number, thickness and loading arrangements of GFRP layers at different depths of GLULAM beams, Taheri, Zou *et al.* (2005) has carried out another experiment, showing that arrangement of these reinforcing layers in the middle and lower parts of GLULAM beams has increased their hardness and resistance. Nowadays, plant fibers are commonly used to make composites due to its easily natural cycle and cost-effective. Wood-Plastic composite consists of any shape wood, and plastic in thermosetting or thermoplastics forms. The combination of plastic plates as a FRP-shaped core (fiber reinforced polymer) in its upper and lower parts creates a sandwich panel Wechsler and Hiziroglu (2007). By the raise of reinforcement layers' number, final load has not been dramatically increased because the core section is very weak in comparison with the surface. Also, prior to the surfaces activation, the shear force created in the core and placed under the point-load has caused the rupture in the area. In the same vein, Lale Arefi *et al.* (2014) and Naghipour, Nematzadeh *et al.* (2011) have carried out another laboratory investigation, suggesting that the formation of a groove with a specific depth would cause reinforcing plates to reach their maximum carrying capacity and fully avoided separation between the core and reinforcement layers. Also, increasing the number of reinforcing layers has increased the hardness and flexural strength of the composite sections. In this research, wooden columns in rectangular and cylindrical geometric shapes have been reinforced by different hollow sections with variable connection types. The goal of this laboratory research is to choose the most appropriate method to increase the ultimate load carrying capacity and ductility of composite sections.

2. Laboratory testing program

2.1 Material properties and specimens

In this study, 13 sample groups under the axial load pressure have been tested to determine their load capacity and ductility. The specimens consist of rectangular hollow steel sections of 0.32 and 0.4 mm thick sheets with the edges of two ends that are accurately raised 1 cm. The process is to achieve consistency and greater accuracy in test results. Specimens of group 1 are wooden timber cut in 6.2×6.2 and 20 cm high. The specimens in group2 are rectangular hollow steel sections with a thickness of 0.32 mm attached together by adhesive. In this research, due to the use of connecting timbers with rectangular steel tubes varies (method), adhesives and screws have been used. The number and spacing of the screws and thickness of steel sheets are the key factors in load capacity and ductility of samples. In this test, epoxy adhesive of Sicator is used, including two parts as resin and hardening to connect some other specimen with a 3mm diameter screw (Table 1). To

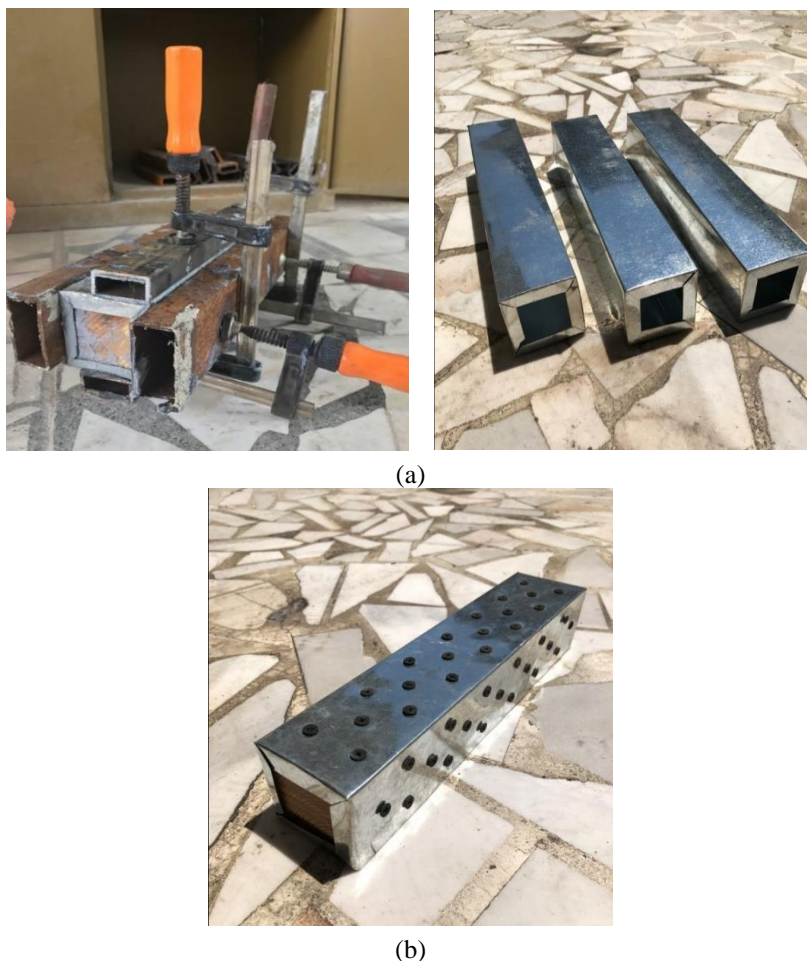


Fig. 1 (a) adhesive joint mounted and fitted of hollow steel section and timber using a clamp; (b) Composite section formed by screw connections

ensure that the adhesive is completely set and the sheets of steel are placed perfectly uniformly on the wooden sheet (Fig. 1a), clamps are used on the four sides of the specimens. The time required to reach the maximum adhesive strength is 7 to 10 days, and before testing all the specimens, they have been kept at a temperature of 24 ° C for one week to gain the desired adhesiveness, letting the steel plate and wood completely be connected, and to prepare the compound section. In order to compare the specimens of group 3, the rectangular sections of hollow steel with a thickness of 0.4 mm are bonded to the wooden timbers by adhesive. Following Fig. 1(b), in groups 4, 5 and 6, the rectangular steel sections of 0.32 mm thick are connected to the timber by a screw, except for the fact that 112, 84 and 56 screws are respectively used for joining them. Fig. 2 shows that in group 7, 8 and 9 specimens, timbers are connected to FRP sheet using adhesive. The difference is the direction in which the sheets are placed. The fibers of the sheets are vertically located at 0, 45 and 90 degrees to the right, and covered the timber. All information about the specimens and their properties are given in Table 2.

2.2 Standard specimens

In this study, according to the compressive strength of the composite specimen which contains steel and concrete,

Table 1 Property of epoxy resins

Special weight (Kg/m ³)	Compressive strength (MPa)	Flexural strength (MPa)	Tensile strength (MPa)
1400	60	40	20



Fig. 2 Rectangular timber columns confined with FRP sheets



Fig. 3 Standard steel sections

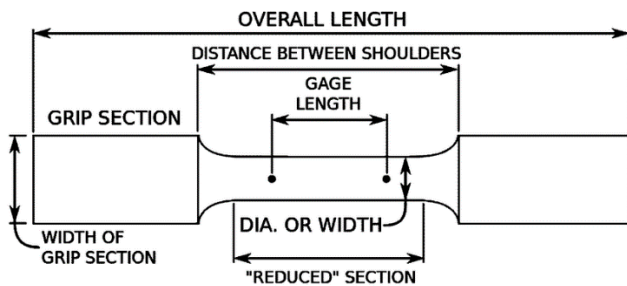


Fig. 4 Details of standard specimen

Table 2 Different specimens and specification

Specimens	Description
Sample group U1	Unconfined rectangular timber
Sample group T1	Rectangular steel tubes (0.32mm) were attached to timber by adhesive.
Sample group T2	Rectangular steel tubes (0.4 mm) were attached to the timber by adhesive.
Sample group B1	Rectangular steel tubes (0.32 mm) were attached to timber by 112 bolts.
Sample group B2	Rectangular steel tubes (0.32 mm) were attached to timber by 84 bolts.
Sample group B3	Rectangular steel tubes (0.32 mm) were attached to timber by 56 bolts.
Sample group F1	Rectangular timbers were confined with FRP sheets and their fibers were placed perpendicularly at a 0 degree angle.
Sample group F2	Rectangular timbers were confined with FRP sheets and their fibers were placed perpendicularly at a 45 degree angle.
Sample group F3	Rectangular timbers were confined with FRP sheets and their fibers were placed perpendicularly at a 90 degree angle.

this relation can be generalized for steel sections and timbers tested. Hence the standard timber columns are cut in dimensions of 5.1×5.1 and 20.3 cm high. On the other hand, according to ASTM-E8M, standard steel specimens are cut in specific dimension for tensile test (Fig. 3 and Fig. 4) (Table 3).

Table 3 Details of standard steel specimens in this test

Width of grip section	Grip section	Distance between shoulders	Overall length	Radius	Width	Gage length
0.95	3.175	3.175	10.16	0.635	0.635	3.175



Fig. 5 Testing apparatus

2.3 Test setup

All specimens are loaded by STM400 device at 2 mm / min speed under a compressive axial load at the structural laboratory of the Babol Noshirvani University of Technology. The machine has been connected to a data acquisition system, whereby all the required data has been processed and filled so that the required data is subsequently readily accessible. Loading of specimens is continued until they tolerated the maximum axial load capacity and the slope of the force-displacement curve reduced to 20% of maximum final resistance. Fig. 5 shows how the specimens were placed on the device. In this study, the proper and high ductility of composite sections means that the ultimate load carrying capacity has not caused the wood to crack and expand, and the composite beam joints have not been detached.

3. Observations and findings

Laboratory results of displacement, loading and crack expansion recorded at different stages of loading are as follows:

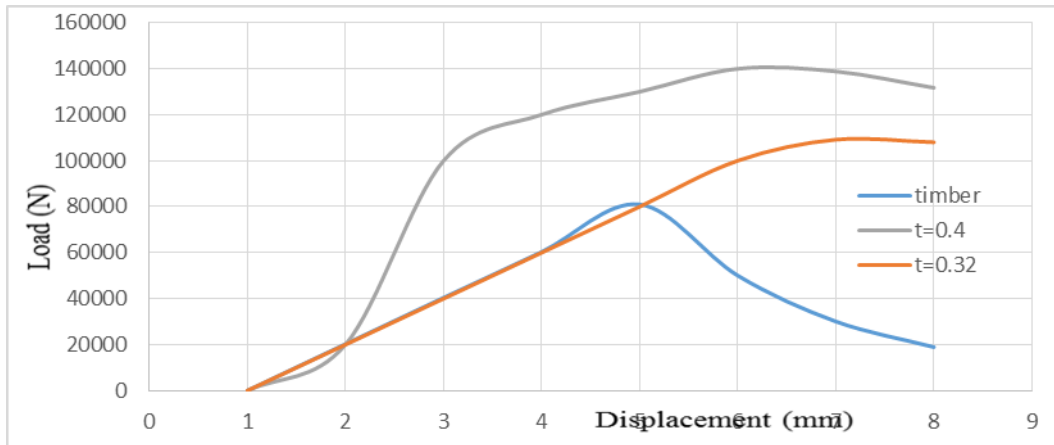


Fig. 6 Comparison between unconfined and confined rectangular specimens with hollow steel sections using adhesive joints

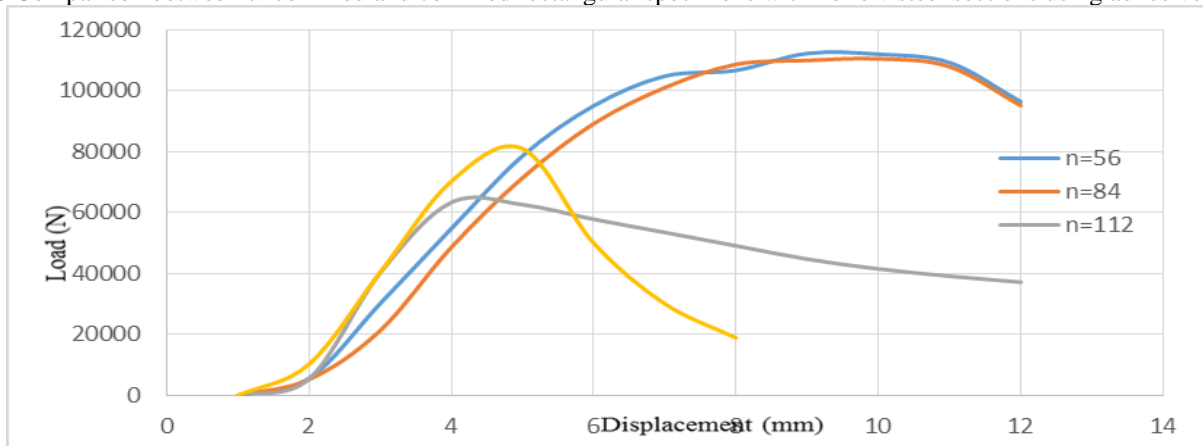


Fig. 7 Rectangular specimens confined with hollow steel sections connected by screws

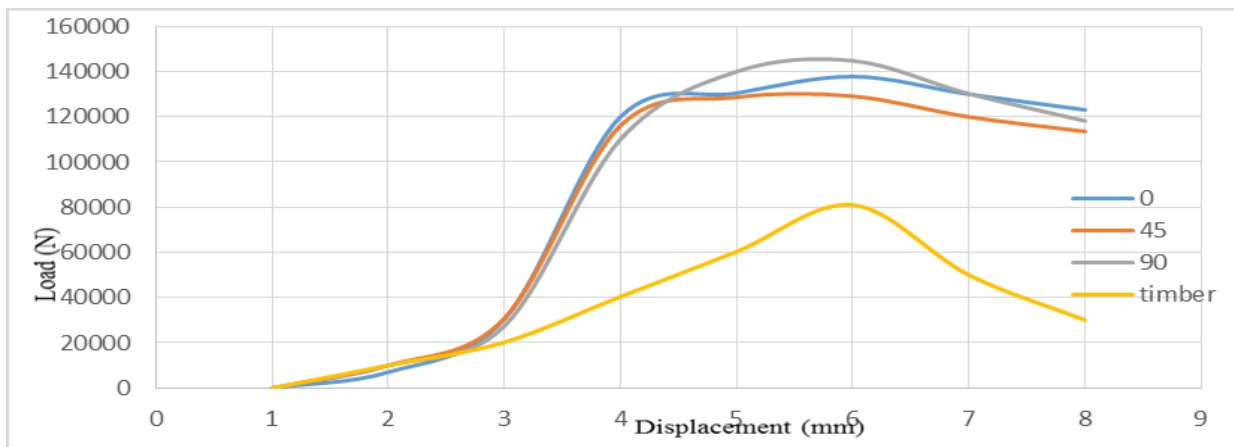


Fig. 8 Rectangular specimens reinforced with FRP polymers

3.1 Effect of confinement with rectangular hollow steel sections which were connected by epoxy resins:

Unconfined timbers have diagonal cracks in their near top area and have low ductility, however, according to Fig. 6, they have resisted about 9 tons. By confining this timber with a hollow rectangular steel section of 0.32 mm thick, the ductility has been significantly increased. However, these resistant composites have tolerated about 11 tons, and have not shown much reduction in resistance even a long time after applying the load. By confining timbers with 0.4 mm thick steel sections, the shape and load capacity

of the section has been dramatically increased and resisted a load of 14 tons (roughly).

There are ruptures between steel sections and timbers on the edges of specimens in group 2 and 3. The diagonal cracks of confined and rupture in unconfined specimens are shown in Fig. 9. (a) and (b).

3.2 Effect of confinement with rectangular hollow steel sections connected by screws:

Specimens in groups 4, 5 and 6 are different in the number of connecting screws. According to Fig. 7, test



(a)



(b)

Fig. 9 (a) Unconfined rectangular specimens. (b) Confined rectangular specimens

results on these specimens are similar to the number of screws reductions, and the load-bearing capacity of samples is increased (Fig. 10). In group 4 specimens, due to the large number of screws and high stress concentration, the resistance is about 6 tons and this group has not shown high ductility. The specimens in group 5 have shown resilience about 11 tons and the resistance in group 6 is about 11.8 tons, however, both samples show good ductility.

3.3 Rectangular specimens reinforced with FRP polymers:

The difference in the specimens in groups 7, 8 and 9 is in the direction of placing the reinforced polymer fibers to the vertical plane. According to Fig. 11 and Fig. 8, specimens in groups 7 and 8 both resisted about 13.4 tons, and few thin cracks appeared in the upper and lower parts of these specimens, however, in the middle part of group 7, some diagonal cracks have been occurred.

Group 9 specimens has a higher load-bearing capacity than the previous two groups with a resistance of about 14.8 tons. These sections shows a better ductility (Fig. 12) and has only a small horizontal crack near the top part.

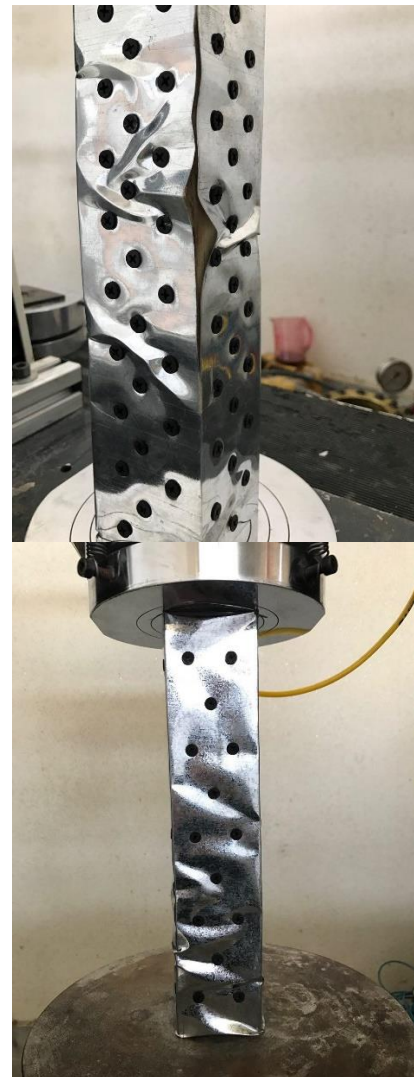


Fig. 10 The effect of reduction in screws number

4. Weight ratios and discussions

In this study, ω is the weight ratio of confined timber columns which is obtained from the weight difference of confined and unconfined samples divided by the weight of sole timbers without any confinement. Furthermore, parameter ρ is defined as the ratio of resistance, which is the difference of ultimate load capacity of confined and unconfined specimens divided by the sole timber without any confinement. It can be seen that, confinement with rectangular steel tubes and epoxy adhesive brought about the weight has been increased 41%, while 56% of capacity is obtained. In confinement with rectangular steel tubes and screws, the weight has been averagely increased by 36%, while the strength capacity growth is 42%. Finally, in timber columns confined with CFRP sheets, the weight has been increased on average only 12%, while there is a significant increment in capacity about 72%. It indicates that CFRP confinement has provided an additional capacity of around three-quarter of sole timber columns without any confinement for composite specimens. The two aforementioned parameters are also plotted as a bar chart in Fig. 13.

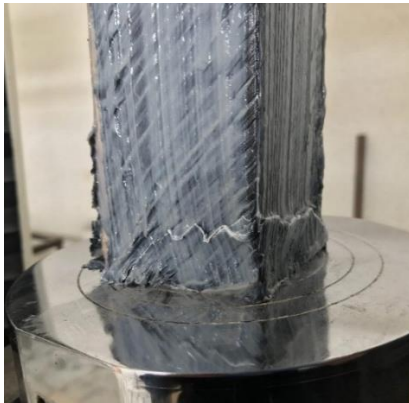


Fig. 11 Small cracks in groups 7 and 8, b. Diagonal cracks in group 8



Fig. 12 Cracks in group 9

5. Timber confinement coefficient in composite specimens

5.1 Compressive strength of composite specimens under the axial load

This section consists of the rolled steel sheet while covering the concrete and due to the adequate cohesion with each other could perform simultaneously, or are compressive steel components filled with concrete. Moreover, according to the plastic-stress distribution method, the nominal strength of the members is determined. To determine the axial pressure and moment of concrete filled steel profiles, the sections have been classified to three types: compressed, semi-compressed and non-compressed sections, which the width to thickness ratio of components can be useful. The compressive design strength of complex section axial members surrounded in concrete is equal to $P_n \times \phi_c$ while ϕ_c is the reduction strength coefficient equal to 0.75 and P_n is the nominal compressive strength that must be determined according to the limit states of buckling concerning column slenderness:

$$\text{For } \frac{P_n 0}{p_e} < 2.25 :$$

$$P_n = P_n 0 \times \left(0.685 \frac{P_n 0}{p_e} \right)$$

$$\text{For } \frac{P_n 0}{p_e} > 2.25 :$$

$$P_n = 0.877 \times P_e$$

In the above aforementioned equations:

$$P_n = (F_y \times A_s) + (F_{ysr} \times A_{sr}) + (0.85 \times F_c \times A_c)$$

$$P_e = \pi^2 \times \left\{ \frac{[EI(eff)]}{(KL)^2} \right\}$$

A_c = Concrete area

A_s = Steel cross section

A_{sr} = Total area of longitudinal rebar

E_c = Modulus elasticity of concrete

F_{ysr} = Yield tension of longitudinal rebar

$EI_{(eff)}$ = effective rigidity of complex section

K = effective length coefficient of the axial member

L = free length of axial member (without lateral restraint)

F_c = Compressive strength of concrete cylindrical specimens (Ghanbari Ghazijahani, Jiao *et al.* 2015)

5.2 Standard specimens load bearing capacity

5.2.1 Standard timber columns

As it is shown in Fig. 14, standard timber columns without any confinement has a load bearing capacity around 7 ton, while they have shown a low ductility. At the bottom of these specimens, a diagonal crack has been occurred (Fig. 16).

5.2.2 Standard steel specimens under the tensile test

Geometry and details of these specimens are given to the computer which is connected to STMctrlr device (Fig. 17). After the test, specimens have shown an ultimate tensile strength around 0.04 ton while they ruptured at the middle. The machine also has provided a force-displacement curve (Fig. 15).

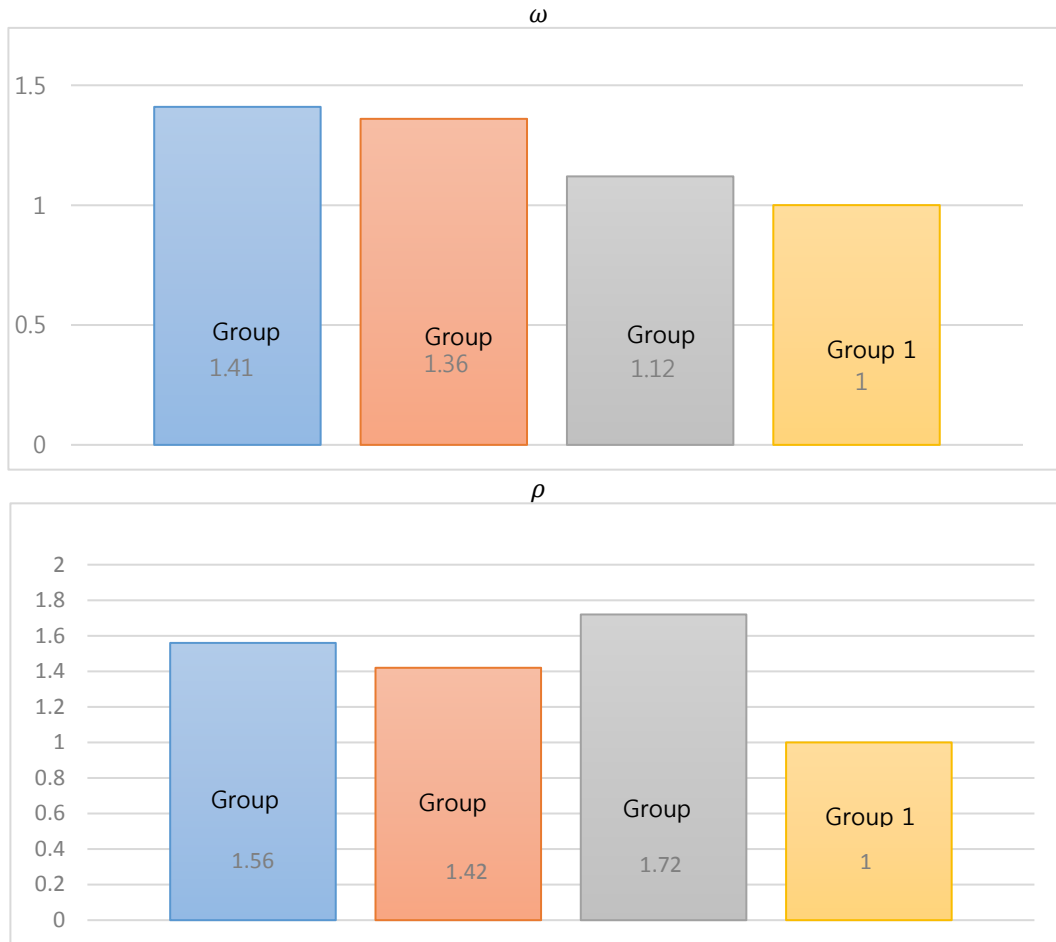


Fig. 13 Weight and strength ratio

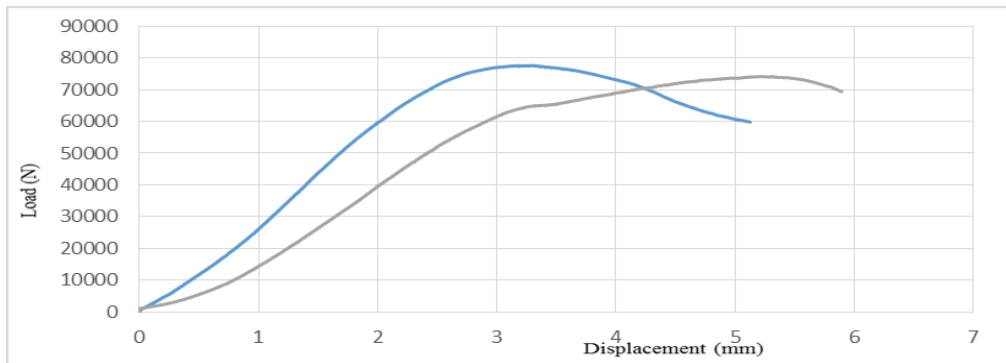


Fig. 14 Standard timber columns under compression

5.3 Coefficient of timber specimens

According to the compressive strength of the composite specimen which contains steel and concrete, this relation can be generalized for the steel sections and timbers tested in this study. Therefore, according to the information obtained from this study, the coefficient of timber confinement is obtained in relation to the compressive strength of the composite cross sections consisting of timber and rectangular steel tubes or FRP sheets:

$$P_{cr} = (A_s \times F_y) + [\alpha \times (F_{yw} \times A_w)]$$

P_{cr} = Compressive strength of composite sections
 A_s = Steel area

F_y = Yield tension of steel sheets

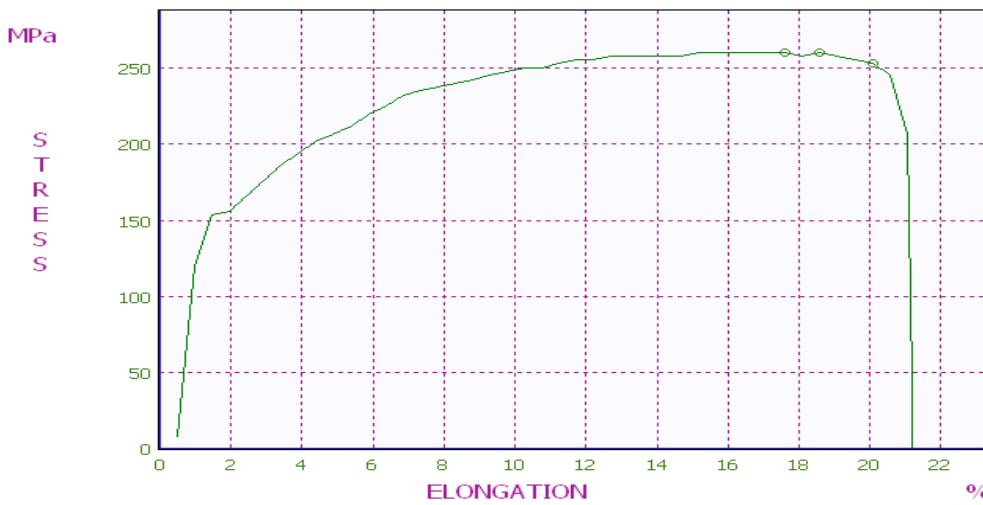
α = Timber confinement coefficient

F_{yw} = Timber yield tension which is obtained from the load bearing capacity of wooden columns divided by wooden area

A_w = Timber area

STMctrlr
STM Series Machine Control And Report Software

SANTAM
ENG. DESIGN CO. LTD.
Tel: 66806397, 66814497, 66814498
Fax: 66816581 Tehran-IRAN



Specifications		[SI]
Customer:	1	
Operator:	MAJIDI	
Date:	2018/04/15	
--- Sample ID:	CU	
Section type:	Rectangular	
Thickness:	0.4 (mm)	
Width:	6 (mm)	
Gauge length:	32 (mm)	
--- Speed:	2 (mm/min)	

Tensile Test

Results	Force (N)	Extension (mm)	Stress (MPa)	Elongation (%)	Elong. Aft.Brk (%)	Module (MPa)	Energy (J)	Bending St. (MPa)	Time (Min)
Peak	626.4	5.9495	260.5833	18.5922	12.34111	1401.573	3144.359	31.3 k	0
Break	607	6.4176	252.9167	20.055	14.00133	1261.115	3432.797	30.4 k	0
Yield	625.4	5.6378	260.5833	17.6181	11.36701	1479.066	2950.365	31.3 k	0

Comments

Fig. 15 Result of the Standard tensile test

All the information related to these parameters is obtained in this experiment which can be put into the equation, thus α as the confinement coefficient can be calculated.

5.3.1 Timber confinement coefficient in T1 specimens:

$$Pcr = (As \times Fy) + [\alpha \times (Fyw \times Aw)]$$

$$Pcr = 11 \text{ ton}$$

According to the rupture force and splitting standard, the specimen are built of steel sheet, the yield stress of steel determines.

$$As = 4 \times (b \times t) = 4 \times (62 \times 0.32) = 79.36 \text{ mm}^2$$

$$Fys = 155 \text{ MPa} = 0.015 \frac{\text{ton}}{\text{mm}^2}$$

Besides, the wood's yield strength calculates the concerning rupture force and wooden specimen area.

$$Aw = b \times t = 62 \times 62 = 3844 \text{ mm}^2$$

$$Fyw = \frac{Pcrw}{Aws} = \frac{Pcrw}{(b \times t)} = \frac{7}{(52 \times 52)} = 0.002 \text{ ton/mm}^2$$

$$11 = (79.36 \times 0.015) + (\alpha \times 3833 \times 0.0022)$$

$$\alpha = 1.16$$

5.3.2 Timber confinement coefficient in T2 specimens:

$$Pcr = (As \times Fy) + [\alpha \times (Fyw \times Aw)]$$

$$Pcr = 14 \text{ ton}$$

$$As = 4 \times (62 \times 0.4) = 99.2 \text{ mm}^2$$

$$Fys = 155 \text{ MPa} = 0.015 \frac{\text{ton}}{\text{mm}^2}$$

$$Aw = 62 \times 62 = 3844 \text{ mm}^2$$

$$Fyw = \frac{7}{(52 \times 52)} = 0.002 \frac{\text{ton}}{\text{mm}^2}$$

$$Pcr = (As \times Fy) + [\alpha \times (Fyw \times Aw)]$$

$$14 = (99.2 \times 0.015) + (\alpha \times 3844 \times 0.002)$$

$$\alpha = 1.62$$

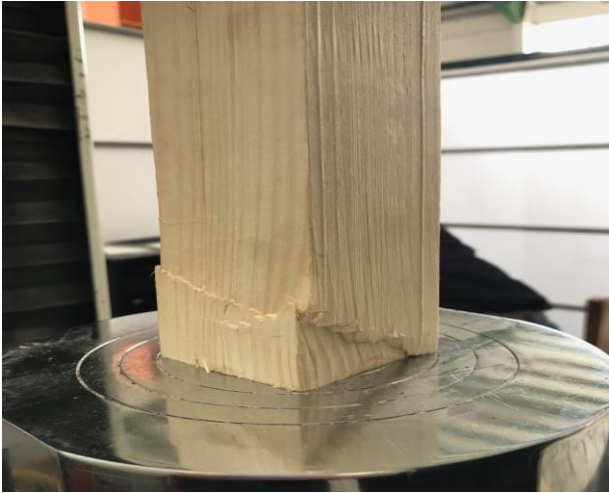


Fig. 16 Cracks in standard timber columns



Fig. 17 Standard tensile test

5.3.3 Timber confinement coefficient in G1 specimens:

$$P_{cr} = (A_s \times F_y) + [\alpha \times (F_{yw} \times A_w)]$$

$$P_{cr} = 6.2 \text{ ton}$$

$$A_s = 4 \times (62 \times 0.32) = 79.36 \text{ mm}^2$$

$$F_{ys} = 155 \text{ MPa} = 0.015 \frac{\text{ton}}{\text{mm}^2}$$

$$A_w = 62 \times 62 = 3844 \text{ mm}^2$$

$$F_{yw} = \frac{7}{(52 \times 52)} = \frac{0.002 \text{ ton}}{\text{mm}^2}$$

$$P_{cr} = (A_s \times F_y) + [\alpha \times (F_{yw} \times A_w)]$$

$$6.2 = (79.36 \times 0.015) + [\alpha \times (3844 \times 0.002)]$$

$$\alpha = 0.65$$

5.3.4 Timber confinement coefficient in G2 specimens:

$$P_{cr} = (A_s \times F_y) + [\alpha \times (F_{yw} \times A_w)]$$

$$P_{cr} = 11 \text{ ton}$$

$$A_s = 4 \times (62 \times 0.32) = 79.36 \text{ mm}^2$$

$$F_{ys} = 155 \text{ MPa} = 0.015 \frac{\text{ton}}{\text{mm}^2}$$

$$A_w = 62 \times 62 = 3844 \text{ mm}^2$$

$$F_{yw} = \frac{7}{(52 \times 52)} = \frac{0.002 \text{ ton}}{\text{mm}^2}$$

$$P_{cr} = (A_s \times F_y) + [\alpha \times (F_{yw} \times A_w)]$$

$$11 = (79.36 \times 0.015) + [\alpha \times (3844 \times 0.002)]$$

$$\alpha = 1.27$$

5.3.5 Timber confinement coefficient in F1 specimens:

In this study, the yield stress of fiber reinforced polymer sheets is about 417 MPa that can be used as F_y (yield strength) in compressive strength of the composite specimen relation and the timber confinement coefficient can be calculated.

$$P_{cr} = 13.8 \text{ ton}$$

$$A_s = 4 \times (62 \times 0.32) = 79.36 \text{ mm}^2$$

$$F_y(frp) = 0.04 \frac{\text{ton}}{\text{mm}^2}$$

$$A_w = 62 \times 62 = 3844 \text{ mm}^2$$

$$F_{yw} = \frac{7}{(52 \times 52)} = \frac{0.002 \text{ ton}}{\text{mm}^2}$$

$$P_{cr} = (A_s \times F_y) + [\alpha \times (F_{yw} \times A_w)]$$

$$13.8 = (79.36 \times 0.04) + [\alpha \times (3844 \times 0.002)]$$

$$\alpha = 1.38$$

5.3.6 Timber confinement coefficient in F2 specimens:

$$P_{cr} = 13 \text{ ton}$$

$$A_s = 4 \times (62 \times 0.32) = 79.36 \text{ mm}^2$$

$$F_y(frp) = 0.04 \frac{\text{ton}}{\text{mm}^2}$$

$$A_w = 62 \times 62 = 3844 \text{ mm}^2$$

$$F_{yw} = \frac{7}{(52 \times 52)} = \frac{0.002 \text{ ton}}{\text{mm}^2}$$

$$P_{cr} = (A_s \times F_y) + [\alpha \times (F_{yw} \times A_w)]$$

$$13 = (79.36 \times 0.04) + [\alpha \times (3844 \times 0.002)]$$

$$\alpha = 1.27$$

5.3.7 Timber confinement coefficient in F3 specimens:

Table 4 Confinement coefficient for different specimens

Specimens	G1	G2	B1	B2	B3	F1	F2	F3
Coefficient	1.16	1.62	0.65	1.27	1.27	1.38	1.27	1.51

$$P_{cr} = 14.8 \text{ ton}$$

$$A_s = 4 \times (62 \times 0.32) = 79.36 \text{ mm}^2$$

$$F_y(frp) = 0.04 \frac{\text{ton}}{\text{mm}^2}$$

$$A_w = 62 \times 62 = 3844 \text{ mm}^2$$

$$F_{yw} = \frac{7}{(52 \times 52)} = \frac{0.002 \text{ ton}}{\text{mm}^2}$$

$$P_{cr} = (A_s \times F_y) + [\alpha \times (F_{yw} \times A_w)]$$

$$14.8 = (79.36 \times 0.04) + [\alpha \times (3844 \times 0.002)]$$

$$\alpha = 1.51$$

As a result, the confinement coefficient of timber for specimens confined with rectangular steel tubes or FRP sheets with the help of adhesive or bolts are shown in Table 4.

6. Conclusion

Reinforced sections can be used in new buildings or reinforcing applications to increase the final load-bearing capacity and the ductility of composite columns. Different methods of reinforcing timbers have been described and the sections are placed under axial load. Based on experimental results of this study, the following conclusion can be drawn:

(1) According to the results of experiments, among the specimens confined with rectangular steel tubes joined together by adhesive, those confined with 0.4 mm thickness steel sections adds a considerable axial resistance.

(2) According to the test on confined specimens with hollow steel sections connected by screws, it can be concluded that the sections connected with 56 screws have shown more resistance. The specimens in group 3 is outperformed in both resistance and ductility.

(3) Among the rectangular specimens reinforced with FRP sheets, those whose fibers are placed at 90 degrees perpendicular to the surface has better load-bearing capacity with better ductility. Finally, by comparing of groups 3 and 9, it can be concluded that reinforcement with FRP sheets has been significant.

(4) In all samples, especially groups 7, 8 and 9, the strength capacity has been raised significantly and exceeded the weight ratios.

(5) The coefficient of timber confinement, enclosed by rectangular steel tubes with 0.4 mm thickness and connected by adhesive, is higher than other composite sections and equals 1.62, which all shows the importance of timber reinforcement with steel tubes that can be applied in wood industry to reinforce timbers.

7. Data Availability

The data that support the findings of this study are available from the first author, upon reasonable request.

References

- Abedini, M., Khlghi, E. A., Mehrmashhadi, J., Mussa, M. H., Ansari, M. and Momeni, T. (2017), "Evaluation of Concrete Structures Reinforced with Fiber Reinforced Polymers Bars: A Review", *J. Asian Scientific Res.*, 7(5), 165-175. <https://doi.org/10.18488/journal.2.2017.75.165.175>.
- Austin, C. D. (2003), *Buckling of Symmetric Laminated Fiberglass Reinforced (FRP) Plates*, University of Pittsburgh.
- Chen, T., Qi, M., Gu, X. L. and Yu, Q. Q. (2015), "Flexural Strength of Carbon Fiber Reinforced Polymer Repaired Cracked Rectangular Hollow Section Steel Beams", *J. Polymer Sci.*, 2015, 9. <https://doi.org/10.1155/2015/204861>.
- de Oliveira, W. L. A., De Nardin, S., de Cresce El, A. L. H. and El Debs, M. K. (2009), "Influence of concrete strength and length/diameter on the axial capacity of CFT columns", *J. Construct. Steel Res.* 65(12), 2103-2110. <https://doi.org/10.1016/j.jcsr.2009.07.004>.
- Eshaghian, M. and A. Keramati (2017), "Experimental and Numerical Study of GFRP Composite Columns with Concrete infill", *Scientific Res. J. (Structural Engineering and Construction)*, 139-147.
- Gerami, M., Bazzaz, M., Andalib, Z. and Bazzaz, M. (2008), "Retrofit of Reinforced Concrete Frame with Steel Bracing System", *14th International Civil Engineering Student Conference. Semnan, Iran*, 14, 1-17.
- Ghazijahani, T.G., Jiao, H. and Holloway, D. (2015), "Rectangular steel tubes with timber infill and CFRP confinement under compression: Experiments", *J. Construct. Steel Res.* 114, 196-203. <https://doi.org/10.1016/j.jcsr.2015.07.015>.
- Han, L.H., Yao, G.H. and Tao, Z. (2007), "Performance of concrete-filled thin-walled steel tubes under pure torsion", *Thin Wall. Struct.* 45(1), 24-36. <https://doi.org/10.1016/j.tws.2007.01.008>.
- Hosseinpour, E., Baharom, S., Badaruzzaman, W. H. W., Shariati, M. and Jalali, A. (2018), "Direct shear behavior of concrete filled hollow steel tube shear connector for slim-floor steel beams", *Steel Compos. Struct.*, 26(4), 485-499. <https://doi.org/10.12989/scs.2018.26.4.485>.
- Khanouki, M. A., Sulong, N. R., Shariati, M. and Tahir, M. M. (2016), "Investigation of through beam connection to concrete filled circular steel tube (CFCST) column", *J. Construct. Steel Res.*, 121, 144-162. <https://doi.org/10.1016/j.jcsr.2016.01.002>.
- Lale Arefi, S., Naghipour, M., Turskis, Z. and Nematzadeh, M. (2014), "Evaluation of grooving method to postpone debonding of FRP laminates in WPC-FRP beams", *J. Civil Eng. Management*, 20(2), 237-246. <https://doi.org/10.3846/13923730.2013.878379>.
- Lee, S. H., Kim, S. H., Bang, J. S., Won, Y. A. and Choi, S. M. (2011), "Structural Characteristics of Welded Built-up Square Concrete Filled Tubular Stub Columns Associated with Concrete Strength", *Procedia Eng.*, 14, 1140-1148. <https://doi.org/10.1016/j.proeng.2011.07.143>.
- Luo, Z., Sinaei, H., Ibrahim, Z., Shariati, M., Jumaat, Z., Wakil, K., Phram, B.T., Mohamad, E.T. and Khorami, M. (2019), "Computational and experimental analysis of beam to column joints reinforced with CFRP plates", *Steel Compos. Struct.* 30(3), 271-280. <https://doi.org/10.12989/scs.2019.30.3.271>.
- Mehrmashhadi, J., Chen, Z., Zhao, J. and Bobaru, F. (2019), "A stochastically homogenized peridynamic model for intraply fracture in fiber-reinforced composites", *Compos. Sci. Technol.*

107770. <https://doi.org/10.1016/j.compscitech.2019.107770>.
- Naghipour, M., Nematzadeh, M. and Yahyazadeh, Q. (2011), "Analytical and experimental study on flexural performance of WPC-FRP beams", *Construct. Build. Mater.*, **25**(2), 829-837. <https://doi.org/10.1016/j.conbuildmat.2010.06.104>.
- Paknahad, M., Bazzaz, M. and Khorami, M. (2018), "Shear capacity equation for channel shear connectors in steel-concrete composite beams", *Steel Compos. Struct.* **28**(4), 483-494. <https://doi.org/10.12989/scs.2018.28.4.483>.
- Raftery, G. M. and F. Kelly (2015), "Basalt FRP rods for reinforcement and repair of timber", *Compos. Part B Eng.* **70**, 9-19. <https://doi.org/10.1016/j.compositesb.2014.10.036>.
- Rashidi, M. and H. Takhtfrouzeh (2018), "An Experimental Study on Shear and Flexural Strengthening of Concrete Beams Using GFRP Composites", *J. Integrated Eng.*, **3**(1), 1-7.
- Sajedi, F. and M. Shariati (2019), "Behavior study of NC and HSC RCCs confined by GRP casing and CFRP wrapping", *Steel Compos. Struct.*, **30**(5), 417-432. <https://doi.org/10.12989/scs.2019.30.5.417>.
- Sedghi, Y., Zandi, Y., Toghroli, A., Safa, M., Mohamad, E. T., Khorami, M. and Wakil, K. (2018), "Application of ANFIS technique on performance of C and L shaped angle shear connectors", *Smart Struct. Syst.* **22**(3), 335-340. <https://doi.org/10.12989/sss.2018.22.3.335>.
- Shariati, M., Tahir, M. M., Wee, T. C., Shah, S. N. R., Jalali, A. and Khorami, M. (2018), "Experimental investigations on monotonic and cyclic behavior of steel pallet rack connections", *Eng. Failure Anal.* **85**: 149-166. <https://doi.org/10.1016/j.engfailanal.2017.08.014>.
- Sinaei, H., Jumaat, M. Z. and Shariati, M. (2011), "Numerical investigation on exterior reinforced concrete Beam-Column joint strengthened by composite fiber reinforced polymer (CFRP)," *J. Physical Sci.* **6**(28), 6572-6579. <https://doi.org/10.5897/IJPS11.1225>.
- Taheri, F., Zou, G. P. and Naghipour, M. (2005), "Experimental and theoretical investigations into the energy absorption response of GFRP-strengthened glulam beams under impact loading", *Forest Products J.*, **55**(4), 62-71.
- Toghroli, A., Darvishmoghaddam, E., Zandi, Y., Parvan, M., Safa, M., Abdullahi, M. A. M. Heydari, A., Wakil, K., Gebreel, S.A.M. and Khorami, M. (2018), "Evaluation of the parameters affecting the Schmidt rebound hammer reading using ANFIS method", *Comput. Concrete*, **21**(5), 525-530. <https://doi.org/10.12989/cac.2018.21.5.525>.
- Wechsler, A. and S. Hiziroglu (2007), "Some of the properties of wood-plastic composites", *Build Environ.*, **42**(7), 2637-2644. <https://doi.org/10.1016/j.buildenv.2006.06.018>.
- Xie, Q., Sinaei, H., Shariati, M., Khorami, M., Mohamad, E.T., Bui, D.T. (2019), "An experimental study on the effect of CFRP on behavior of reinforced concrete beam column connections", *Steel Compos. Struct.*, **30**(5), 433-441. <https://doi.org/10.12989/scs.2019.30.5.433>.
- Zeghiche, J. (2013), "Further tests on thin steel and composite fabricated stubs", *J. Construct. Steel Res.*, **81**, 124-137. <https://doi.org/10.1016/j.jcsr.2012.11.006>.
- Zhao, J., Chen, Z., Mehrmashhadi, J. and Bobaru, F. (2018), "Construction of a peridynamic model for transient advection-diffusion problems", *J. Heat Mass Transfer*, **126**, 1253-1266. <https://doi.org/10.1016/j.jheatmasstransfer.2018.06.075>.